Letter

Learning algorithm reflecting universal scaling behavior near phase transitions

N. Maskara,[1,2,*] M. Buchhold,[1,3] M. Endres,[1] and E. van Nieuwenburg[1,4]

[1]*Division of Physics, Mathematics and Astronomy, California Institute of Technology, Pasadena, California 91125, USA*

[2]*Department of Physics, Harvard University, Cambridge, Massachusetts 02138, USA*

[3]*Institute for Theoretical Physics, University of Cologne, Zülpicher Strasse 77, 50937 Cologne, Germany*

[4]*Niels Bohr International Academy, Niels Bohr Institute, University of Copenhagen, Blegdamsvej 17, 2100 Copenhagen, Denmark*

(Received 12 April 2021; revised 14 December 2021; accepted 15 February 2022; published 9 May 2022)

Machine-learning-inspired techniques have emerged as a new paradigm for analysis of phase transitions in quantum matter. In this work, we introduce a supervised learning algorithm for studying critical phenomena from measurement data, "neural network scaling," which is based on iteratively training convolutional networks of increasing (spatial) complexity and test it on the transverse field Ising chain and $q = 6$ Potts model. At the continuous Ising transition, our scaling procedure directly reflects the hallmark of a continuous (second-order) phase transition, divergence of a characteristic length scale. Specifically, we extract a classification length scale by measuring the response of the classification accuracy while varying the largest convolution size (architecture of the network). We observe empirically the scaling exponent of the classification length is consistent with a power law with the correlation length exponent $\nu = 1$. Furthermore, we demonstrate the versatility of our algorithm by showing the universal scaling behaviors persist across a variety of measurement bases, including when the order parameter is nonlocal. Finally, we show that the classification length scale remains finite for the $q = 6$ Potts model, which has a first-order transition and lacks a divergent correlation length.

DOI: 10.1103/PhysRevResearch.4.L022032

Introduction. Machine learning techniques have emerged as a new tool for analyzing complex many-body systems [1–4]. A particularly well-studied application of such techniques is that of the identification and classification of phase transitions directly from the data, assuming little to no prior knowledge of the underlying physics [5–21]. Typically, the algorithms take as input labeled snapshot measurements of the kind obtained in cold-atom and quantum simulator experiments [22–33]. Recent efforts have expanded such explorations to a diverse range of systems, including disordered [34–37] and topologically ordered systems [38–44], as well as applications to experiments [45–47].

An often-voiced concern, however, is that machine learning methods appear as a black box and that it is difficult to trust neural network classification without traditional supporting evidence. For example, in the study of phase transitions with machine learning, the phase boundary identified by a conventional approach may be affected by short-distance correlations, which turn out to be irrelevant for the thermodynamic phase of the system [10]. Instead, learning algorithms should ideally focus on characteristic signatures of phase transitions which are insensitive to irrelevant correlations, such as power-law divergences near the critical point of a second-order phase transition.

In this paper we develop a machine learning algorithm inspired by this fundamental feature of critical phenomena, i.e., the emergence of long-distance correlations and scale invariance. We dub this method "neural network scaling," as it systematically analyzes critical behavior near a suspected transition point, using only snapshot data, by scaling the functional form of a neural network and looking at the response of the classification accuracy (see Fig. 1). Specifically, we restrict the architecture so the network can only access patches of the snapshot at a time and then vary the largest patch size. The resulting family of models is similar in architecture to those in Refs. [12,48–51]. Critical scaling for varying patch sizes has also been recently observed in Ref. [52] using connected correlation functions.

Under these conditions we can extract information about the structure of correlations in the underlying data. In particular, our main result is the identification of an emergent *classification* length scale ξ_{net}, which we argue on general grounds reflects the underlying system's correlation length. Thus, for a second-order phase transition, ξ_{net} should diverge at the critical point according to a power law with a universal exponent. We exemplify this on the one-dimensional (1D) transverse field Ising model and see scaling of the classification length consistent with known exponents. In contrast, for a first-order transition in the two-dimensional (2D) $q = 6$ Potts model, we see no scaling of the classification length, in line with expectations.

The learning algorithm proves quite versatile and neither requires prior knowledge of the order parameter nor the mea-

*nmaskara@g.harvard.edu

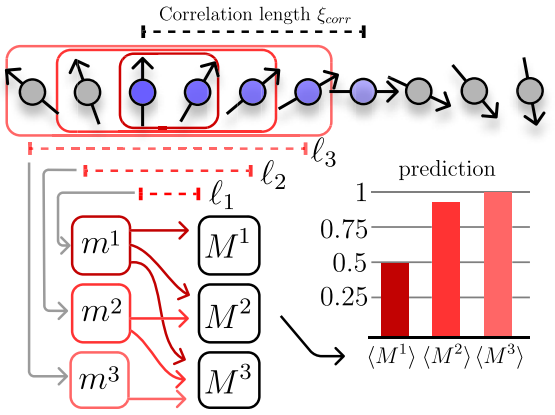

FIG. 1. Conceptual illustration of our method for a 1D spin chain. Snapshots near a second-order phase transition reveal a characteristic length scale ξ_{corr} over which spins are correlated and which diverges at the critical point. The modules m^k are designed to only capture correlations in the data up to a certain length scale ℓ_k, and their outputs are aggregated into M^k. On length scales shorter than ξ_{corr}, the algorithm cannot make a firm distinction between the two phases. As the module size is increased, the prediction $\langle M^k\rangle$ is improved until $\ell_k \sim \xi_{\text{corr}}$, after which it quickly saturates.

surement data. The only information provided is the spatial structure of the measurement data. We demonstrate this versatility by considering data from projective measurements in different measurement bases, without passing the information about the basis to the algorithm. For conventional approaches based on two-site correlation functions or local order parameters, this would make the detection of the thermodynamic phase a tremendous challenge. Nevertheless, the algorithm manages to distinguish the two phases with a high degree of accuracy. This is especially promising in light of studying phase transitions in measurement data, where the generator of the dynamics, i.e., the Hamiltonian or the effective field theory, are unknown. It also provides a promising route to design machine learning approaches to identify phases with nonlocal or hidden order, for which information on the structure of the order parameter or the relevant correlation functions may be unknown or inaccessible.

The algorithm. Neural network scaling is a supervised learning algorithm that systematically adds complexity to a machine learning model. The model is composed of a set of independent computational units, termed *modules*. The algorithm takes and trains modules iteratively, and, by design, each new module learns correlations in the data that the prior modules did not capture. Conceptually, complexity is added by increasing the amount of correlations representable by the model in each step. For any specific application, physical understanding should inform the design of these modules. In this paper the application is to scaling behavior near critical points, so modules are designed to incorporate spatial locality, and each subsequent module captures spatial correlations at a larger length scale.

Each module $m^i : \vec{x} \to \mathbb{R}$, labeled with an index $i = 1, ..., N$, takes as input a snapshot (projective measurement) $\vec{x}$ and maps it to a scalar. Then we apply an aggregation function M^k that aggregates the outputs of the first k modules

Algorithm 1. Iterative training algorithm.

input: Sequence of modules $m^1, ..., m^l$
input: Aggregate models $M^k(m^1, ..., m^k)$, $k \leqslant l$
input: Labeled dataset $\{(\vec{x}_i, y_i)\}$
input: Loss function $\mathcal{L}$
Result: Trained set of models $\{M^k\}$, $k = 1, ..., l$
for $k = 1, ..., l$ **do**
  train M^k on dataset $(\vec{x}_i, y_i)$ by minimizing $\mathcal{L}(y_i, M^k(x_i))$;
  freeze parameters of m^k

$m^1, ..., m^k$, where $k = 1, ..., N$. This results in a sequence of N models $M^k(m^1, ..., m^k)$ with shared modules. In practice, both the modules and the aggregation functions are implemented through a neural network. This model is then trained to minimize a classification loss function $\mathcal{L}$ using the iterative training algorithm described in pseudocode in Algorithm 1.

The intuition behind this algorithm is that the improvement of classification accuracy from model M^k to M^{k+1} can only be due to features captured by module m^{k+1}. Thus in our application the modular architecture along with iterative training allows us to independently learn features at different length scales.

The network. We develop a class of convolutional neural networks for the modules, designed to probe the spatial structure of correlations. Each module m^k takes the functional form

$$m^k(\vec{x}) = \frac{1}{N}\sum_j m_0^k\left(\vec{x}_j^{\ell_k}\right), \tag{1}$$

where m_0^k is a two-layer neural network that acts on a subset $\vec{x}_j^{\ell_k}$ of the data $\vec{x}$. The label ℓ_k indicates the size of a spatial region corresponding to the subset (e.g., ℓ_k adjacent sites in a one-dimensional lattice), and the index j enumerates all N regions of size ℓ_k. Here we have assumed translational invariance, but for systems with boundaries or disorder, the network $m_0^k \to m_j^k$ may also vary from region to region.

The aggregation function we choose is a linear classifier LC, acting on the module outputs $m^k(\vec{x})$:

$$M^K(\vec{x}) = LC(m^1(\vec{x}), m^2(\vec{x}), ...m^K(\vec{x})). \tag{2}$$

The linear classifier is defined by $LC(\{m^i(\vec{x})\}) = \sigma[\sum_i w_i m^i(\vec{x}) - b]$, where σ is the sigmoid function $\sigma(z) = 1/(1+e^{-z})$, and w_i and b are free parameters. The nonlinearity σ maps the linear combination of module outputs to a value between [0,1], as expected for binary classification. The loss function we use is the binary cross entropy, $\mathcal{L}[y_i, M^k(x_i)] = \langle y \log M^k(x_i) + (1-y)\log[1 - M^k(x_i)]\rangle$, where y_i is the target label $y_i \in \{0, 1\}$ and the expectation value is taken over the training dataset.

Choosing a linear classifier ensures that the network cannot capture additional, spurious correlations between regions. A nonlinear classifier may also include products of local correlations like $m^2(\vec{x})m^3(\vec{x})$. These capture *nonlocal* information about potentially disconnected five-site regions, which we exclude on purpose. In the remainder of the text, we use M^ℓ instead of M^K to denote an aggregate classifier with largest convolution length $\ell_K = \ell$.

The full model is naturally represented by a convolutional neural network (CNN). The resulting CNN architecture, with parallel convolutional modules, is similar to the network-in-network architectures from Refs. [12,48,49], the correlation probing neural network from Ref. [50], and to the *EDNN* from Ref. [51]. Our work introduces the idea of scaling convolution size iteratively and observing the response via classification accuracy to extract a characteristic length scale.

Applications. We investigate neural network scaling for a second-order phase transition in the 1D transverse field Ising model (TFIM). The single-parameter Hamiltonian for the 1D TFIM with open boundaries is

$$H(g) = -\sum_{i=1}^{L-1} \sigma_i^z \sigma_{i+1}^z - g \sum_{i=1}^{N} \sigma_i^x, \tag{3}$$

where $\sigma_i^{z,x}$ are Pauli matrices for spin i. At critical value $g_c = 1$, the ground state of this model undergoes a phase transition from a disordered (paramagnetic) to an ordered (ferromagnetic) state, breaking the global $\mathbb{Z}_2$ symmetry. In what follows we focus our attention on a region around $g = g_c$. To construct our dataset, we employ the matrix-product-state-based iTEBD algorithm [53] to numerically determine the ground state as a function of g and sample configurations for a system size of $L = 400$. We then perform projective measurements in multiple bases, including the z basis (measuring σ_i^z on each site), the x basis (measuring σ_i^x), and a few intermediate bases, $\cos(\theta)\sigma_i^z + \sin(\theta)\sigma_i^x$. This illustrates that the classification algorithm does not rely on the *a priori* choice of an optimal basis, which for experimental measurements may be unknown.

Each snapshot is labeled with the phase it is drawn from, with ordered ($g < g_c$) or disordered ($g > g_c$), labeled as 1 or 0, respectively. The machine learning model is trained by minimizing the binary cross entropy between the labels and the prediction $M^\ell(x)$ (see *The Network*), on snapshots drawn from the ground state of $H(g)$ at 85 different values of g with 800 snapshots per g. Points were spread from $g = 0$ to 4.4 but concentrated in the critical region near $g_c = 1$, with a minimum separation of $\Delta g = 0.01$. Module outputs $\langle m^\ell \rangle_g$ and phase classification $\langle M^\ell \rangle_g$ are computed on a separate validation dataset consisting of 200 snapshots per g and with a minimum separation of $\Delta g = 0.002$ in the critical region. (Neural networks were built and trained using the Keras package [54].) Training is fast, as network sizes are small compared to state-of-the-art deep learning tasks, with a single epoch (training once on each snapshot) taking approximately 3 s for the smallest networks ($\ell = 2$) and 24 s for the largest ($\ell = 18$) on a Google Colab GPU instance. Typical training runs require approximately 100 epochs per ℓ. Once the networks are trained, $\langle M^\ell \rangle_g$ measures how accurately the ground state of $H(g)$ can be inferred from local measurements with spatial extent ℓ, and henceforth we call this the classification accuracy.

Empirically, we find the classification accuracy improves as the convolution size ℓ is increased, with the improvement most dramatic for snapshots drawn near g_c, see Fig. 2(a). The continuous sharpening of the classification curve with increasing convolution size is a robust signature of a second-order phase transition. This is because identifying the phase from local measurements is intimately connected to correlations in the ground state. At the critical point, the ordered and disordered phases are indistinguishable, and the system is dominated by fluctuations with a divergent correlation length ξ_{corr}, resulting in an ambiguous prediction $\langle M^\ell \rangle_{g_c} = 0.5$. As g moves away from the critical point, characteristic correlations indicating one of the possible phases build up at distances larger than ξ_{corr}, while shorter distances remain dominated by fluctuations. Since $\xi_{\text{corr}} \sim |g - g_c|^{-\nu}$ decays as a power law, farther from the critical point the classification accuracy improves for fixed ℓ. Similarly, as ℓ is increased, the accuracy of the classification $\langle M^\ell \rangle_g$ will improve, saturating to either 1 or 0 depending on $g < g_c$ or $g > g_c$, respectively. For an infinitely large system, the classification curve approaches a step function as $\ell \to \infty$.

To quantitatively analyze the relationship between the classification and convolution size, we extract a characteristic length scale associated with the improvement of $\langle M^\ell \rangle_g$ via an inverse exponential fit $|\langle M^\infty - M^\ell \rangle_g| \sim \exp(-\ell/\xi_{\text{net}})$, where ξ_{net} is a g-dependent length scale. Specifically, we set M^∞ to 1 in the ordered phase and 0 in the disordered phase, the saturation values in an ideal, infinitely large system. We consider $\ell < 20$, which obtains convincing prediction probabilities for data points with $|g - g_c| \geqslant 0.01$. As our data is for an $L = 400$ chain, this emulates a thermodynamically large system. We also exclude the smallest module ($\ell = 1$), which only captures single-site observables. The resulting fit between $2 \leqslant \ell < 20$ performs well in the z basis (2c). However, in other bases, specifically, the intermediate $\theta = \pi/4$ basis, the classification accuracy exhibits erratic behavior for small ℓ. Nevertheless, at slightly larger $\ell \approx 5$, scaling with ℓ reappears, and the exponential fit extracts a meaningful length scale ξ_{net} capturing the scaling of $\langle M^\ell \rangle_g$.

Near the phase transition we see that the fitted correlation length ξ_{net} diverges as g approaches the critical point g_c and is well described by a power law [Fig. 2(b)]. Remarkably, the power-law scaling of the fitted classification length $\xi_{\text{net}} \sim |g - g_c|^{-\nu_{\text{net}}}$ is consistent with the known exponent for the 1D TFIM, $\nu_{\text{net}} \approx \nu = 1$. This includes other bases where the phases cannot be reliably distinguished from conventional two-point correlation functions [55]. These observations suggest ξ_{net} reflects the underlying correlation length scale independent of measurement basis and hence can be used to robustly probe the growth of correlations near the critical point.

Above, we have assumed g_c is known *a priori*, which is not typically true. However, we could also consider neural network scaling with a different partitioning of the training labels—ordered ($g < \tilde{g}_c$) or disordered ($g > \tilde{g}_c$)—where $\tilde{g}_c$ is not necessarily the true critical point g_c. In such a case, the classification curves $\langle M^\ell \rangle_g$ still reveal information about the correlations in the vicinity of $\tilde{g}_c$. For example, as shown in [55], for $\tilde{g}_c = 1.05$ we see the classification curve stops improving at some finite ℓ. This is consistent with the underlying system having a finite correlation length at $\tilde{g}_c$. Thus if the critical point is unknown *a priori*, one could estimate it by training a sequence of models for various $\tilde{g}_c$ and identifying g_c with the classification curves that continue improving for the largest ℓ, in the spirit of confusion methods for using supervised learning in an unsupervised context [5]. In addition, farther away from g_c the correlation length is smaller so training can

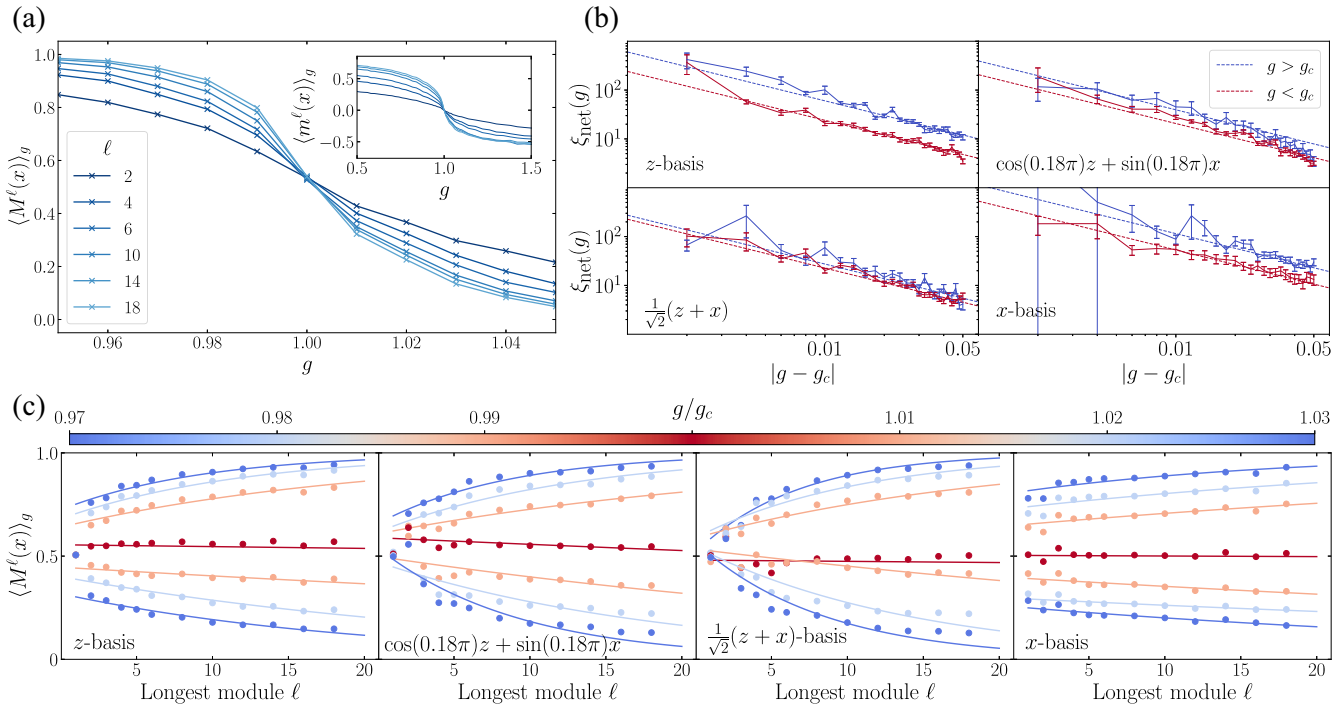

FIG. 2. (a) Average classification $M^\ell(x)$ as a function of the TFIM parameter g and the spatial extent ℓ of the model. Classifiers incorporating longer range correlations can more reliably identify the phase of snapshots taken near the critical point, as evidenced by an increase in the slope. (Inset) Average module outputs $\langle m^\ell\rangle$ also exhibit scaling with ℓ, as one would expect from an order parameter. (b) Fitted classification lengths $\xi_{\rm net}$ on a log-log plot, from measurements in the z (basis $= 0$), x (basis $= \pi/2$), and two intermediate bases $\cos(0.18\pi)z + \sin(0.18\pi)x$ (basis $= 0.18\pi$) and $(z+x)/\sqrt{2}$ (basis $= \pi/4$), plotted on a log-log scale. For each basis, points are separate for approaching g_c from above (blue) or below (red). Data for g near g_c is consistent with power-law behavior with exponent $\mu = 1$, which are depicted by colored dotted lines. Error bars are an estimate of the standard deviation in the fitted $\xi_{\rm net}$. (c) Correlation lengths $\xi_{\rm net}$ are extracted by fitting the classification curves $\langle M^\ell\rangle_g$ for each value of g to an inverse exponential form. Fits are performed for classifiers with the largest module size between $2 \leqslant \ell < 20$ and are shown in the same four bases. Notice that in the intermediate bases, especially $\pi/4$, the classification curves behave erratically at very small ℓ but exhibit scaling at intermediate $\ell > 5$. The resulting length scales extracted by the exponential fits are consistent with universal scaling near the critical point $g \approx g_c$ (b).

be stopped at smaller ℓ, reducing the computational resources required.

To contrast the continuous Ising transition, we also examine the $q = 6$ Potts model. Specifically, we used the metropolis Monte Carlo algorithm with Wolff cluster updates [56] to generate samples for an 80×80 lattice with periodic boundary conditions, drawing 1000 snapshots for every T. This model exhibits a first-order phase transition in temperature (T) and hence does not feature a diverging correlation length [57]. As a result we expect that spatially local measurement data should be sufficient to distinguish the two phases, since there are no long-range critical fluctuations. Indeed, our numerical data reflects this intuition, since the classification $\langle M^\ell\rangle_T$ does not exhibit improvement beyond $\ell = 2$ (Fig. 3), regardless of distance to the transition point. Thus neural network scaling can identify the absence of a divergent correlation length in a first-order phase transition.

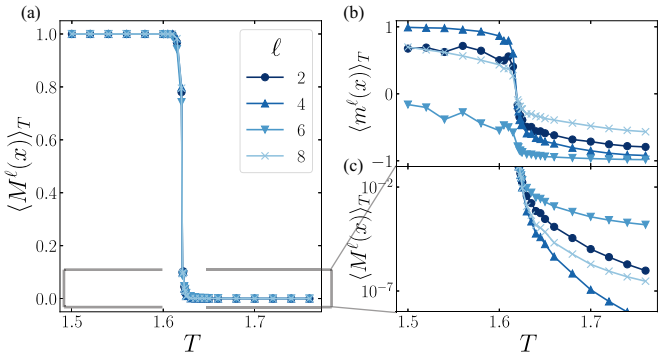

FIG. 3. Potts model data. (a) Predicted classifications $\langle M^\ell\rangle_T$ for the $q = 6$ Potts model do not exhibit scaling with system size, reflecting the fact that the phase transition is first order. (b) The module outputs $\langle m^\ell\rangle_T$, averaged over all snapshots at a given temperature, are in sharp contrast to the second-order transition from Fig. 2. (c) Zooming in on the classifications $\langle M^\ell\rangle_T$ near zero demonstrates the lack of scaling with ℓ.

Discussion. We have presented a flexible method for identifying second-order phase transitions and for extracting a characteristic length scale $\xi_{\rm net}$ directly from measurement data via neural network scaling. Furthermore, $\xi_{\rm net}$ diverges with the same scaling exponent as the physical correlation length $\xi_{\rm corr}$. Above we gave physical arguments for why this occurs, based on indistinguishability of the phase at short distances dominated by critical fluctuations. These arguments are quite general and reflect the emergence of universality at critical points. Indeed, it is widely believed that at the critical point the correlation length $\xi_{\rm corr}$ is the sole contributor to singular,

thermodynamic quantities [58,59]. As long as the model can distinguish the two phases, the classification $\langle M^\ell \rangle_g$ should exhibit a discontinuity at the critical point $g = g_c$ in the thermodynamic limit $\ell \to \infty$, and ξ_{corr} should be the only length scale governing long-distance behavior of $\langle M^\ell \rangle_g$, in agreement with our observations. As such, our scaling procedure makes few assumptions about the microscopic model and could be used to study any system with a continuous phase transition. However, it would be interesting to place our empirical observations on a more rigorous theoretical foundation using the theory of distinguishability near quantum critical points [60,61].

Our analysis of the classification length scale ξ_{net} has been performed for relatively small module sizes $\ell < 20$ compared to the size of the system $L = 400$. This mitigates finite-size effects and yields a scaling of the classification only with the correlation length. However, the method fundamentally cannot know about behaviors at $\ell > 20$. This would be relevant for more subtle cases such as weakly first-order transitions, where new behaviors emerge at larger length scales [62]. Furthermore, in an experimental setting, the maximum correlation length will often be cut off, due to, e.g., adiabatic ramp time or finite system sizes. In such cases there may be multiple relevant length scales for characterizing the classification curves, and a multiparameter scaling analysis could be required. This scenario warrants further study, as it will likely be relevant for near-term quantum simulators, where resources are limited.

The framework presented here for analyzing continuous phase transitions shows more broadly that for classification tasks we can probe an underlying feature of interest by systematically varying the functional form of the models and measuring the response in the form of classification accuracy. In addition to the convolutional neural networks used here, one could consider different classes of models, including kernel methods [8,63] or quantum machine learning models [64,65]. Neural network scaling could also be readily generalized to different kinds of order. For example, dynamical critical exponents could be estimated by looking at time-series data, and using a set of models which can represent observables spanning a finite number of time slices [36,66]. Similarly, phase transitions without conventional order parameters could be studied, perhaps by looking at looplike observables of different sizes [67] or correlations between different snapshots [65,68]. The tools developed here are especially timely, as quantum simulation technologies are rapidly approaching the point where exotic phases of quantum matter can be directly studied in the laboratory.

Acknowledgments. We thank Dolev Bluvstein, Dan Borgnia, Soonwon Choi, Iris Cong, Mikahil Lukin, Brian Timar, Minh Tran, and Ruben Verresen for insightful discussions. N.M. acknowledges funding from a Department of Energy Computational Science Graduate Fellowship under Award No. DE-SC0021110. M.B. acknowledges funding from DFG via Grant No. DI 1745/2-1 under DFG SPP 1929 GiRyd and the CRC network TR 183 (project grant 277101999) as part of project B01. This project has received funding from the European Union's Horizon 2020 Research and Innovation Program under Marie Sklodowska-Curie Grant Agreement No. 847523 INTERACTIONS and Marie Sklodowksa-Curie Grant Agreement No. 895439 "ConQuER."

[1] J. Carrasquilla, Machine learning for quantum matter, Adv. Phys.: X **5**, 1797528 (2020).

[2] P. Mehta, M. Bukov, C.-H. Wang, A. G. R. Day, C. Richardson, C. K. Fisher, and D. J. Schwab, A high-bias, low-variance introduction to machine learning for physicists, Phys. Rep. **810**, 1 (2019).

[3] J. Schmidt, M. R. G. Marques, S. Botti, and M. A. L. Marques, Recent advances and applications of machine learning in solid-state materials science, npj Comput. Mater. **5**, 83 (2019).

[4] G. Carleo, I. Cirac, K. Cranmer, L. Daudet, M. Schuld, N. Tishby, L. Vogt-Maranto, and L. Zdeborová, Machine learning and the physical sciences, Rev. Mod. Phys. **91**, 045002 (2019).

[5] E. van Nieuwenburg, Y.-H. Liu, and S. Huber, Learning phase transitions by confusion, Nat. Phys. **13**, 435 (2017).

[6] J. Carrasquilla and R. G. Melko, Machine learning phases of matter, Nat. Phys. **13**, 431 (2017).

[7] L. Wang, Discovering phase transitions with unsupervised learning, Phys. Rev. B **94**, 195105 (2016).

[8] C. Giannetti, B. Lucini, and D. Vadacchino, Machine learning as a universal tool for quantitative investigations of phase transition, Nucl. Phys. B **944**, 114639 (2019).

[9] P. Ponte and R. G. Melko, Kernel methods for interpretable machine learning of order parameters, Phys. Rev. B **96**, 205146 (2017).

[10] M. J. S. Beach, A. Golubeva, and R. G. Melko, Machine learning vortices at the Kosterlitz-Thouless transition, Phys. Rev. B **97**, 045207 (2018).

[11] K. Liu, J. Greitemann, and L. Pollet, Learning multiple order parameters with interpretable machines, Phys. Rev. B **99**, 104410 (2019).

[12] S. J. Wetzel and M. Scherzer, Machine learning of explicit order parameters: From the Ising model to SU(2) lattice gauge theory, Phys. Rev. B **96**, 184410 (2017).

[13] F. Schäfer and N. Lörch, Divergence of predictive model output as indication of phase transitions, Phys. Rev. E **99**, 062107 (2019).

[14] T. Mendes-Santos, X. Turkeshi, M. Dalmonte, and A. Rodriguez, Unsupervised Learning Universal Critical Behavior via the Intrinsic Dimension, Phys. Rev. X **11**, 011040 (2021).

[15] S. S. Lee and B. J. Kim, Confusion scheme in machine learning detects double phase transitions and quasi-long-range order, Phys. Rev. E **99**, 043308 (2019).

[16] E. Bedolla, L. C. Padierna, and R. Castañeda-Priego, Machine learning for condensed matter physics, J. Phys.: Condens. Matter **33**, 053001 (2021).

[17] M. S. Scheurer and R.-J. Slager, Unsupervised Machine Learning and Band Topology, Phys. Rev. Lett. **124**, 226401 (2020).

[18] R. A. Vargas-Hernández, J. Sous, M. Berciu, and R. V. Krems, Extrapolating Quantum Observables with Machine Learning:

Inferring Multiple Phase Transitions from Properties of a Single Phase, Phys. Rev. Lett. **121**, 255702 (2018).

[19] W. Zhang, J. Liu, and T.-C. Wei, Machine learning of phase transitions in the percolation and X Y models, Phys. Rev. E **99**, 032142 (2019).

[20] J. Greitemann, K. Liu, and L. Pollet, Probing hidden spin order with interpretable machine learning, Phys. Rev. B **99**, 060404(R) (2019).

[21] S. Efthymiou, M. J. S. Beach, and R. G. Melko, Super-resolving the Ising model with convolutional neural networks, Phys. Rev. B **99**, 075113 (2019).

[22] S. Ebadi, T. T. Wang, H. Levine, A. Keesling, G. Semeghini, A. Omran, D. Bluvstein, R. Samajdar, H. Pichler, W. W. Ho *et al.*, Quantum phases of matter on a 256-atom programmable quantum simulator, Nature (London) **595**, 227 (2021).

[23] J. Zhang, G. Pagano, P. W. Hess, A. Kyprianidis, P. Becker, H. Kaplan, A. V. Gorshkov, Z.-X. Gong, and C. Monroe, Observation of a many-body dynamical phase transition with a 53-qubit quantum simulator, Nature (London) **551**, 601 (2017).

[24] F. Arute, K. Arya, R. Babbush, D. Bacon, J. C. Bardin, R. Barends, R. Biswas, S. Boixo, F. G. S. L. Brandao, D. A. Buell, B. Burkett, Y. Chen, Z. Chen, B. Chiaro, R. Collins, W. Courtney, A. Dunsworth, E. Farhi, B. Foxen, A. Fowler *et al.*, Quantum supremacy using a programmable superconducting processor, Nature (London) **574**, 505 (2019).

[25] C. S. Wang, J. C. Curtis, B. J. Lester, Y. Zhang, Y. Y. Gao, J. Freeze, V. S. Batista, P. H. Vaccaro, I. L. Chuang, L. Frunzio, L. Jiang, S. Girvin, and R. J. Schoelkopf, Efficient Multiphoton Sampling of Molecular Vibronic Spectra on a Superconducting Bosonic Processor, Phys. Rev. X **10**, 021060 (2020).

[26] C. Gross and I. Bloch, Quantum simulations with ultracold atoms in optical lattices, Science **357**, 995 (2017).

[27] J.-y. Choi, S. Hild, J. Zeiher, P. Schauß, A. Rubio-Abadal, T. Yefsah, V. Khemani, D. A. Huse, I. Bloch, and C. Gross, Exploring the many-body localization transition in two dimensions, Science **352**, 1547 (2016).

[28] A. Mazurenko, C. S. Chiu, G. Ji, M. F. Parsons, M. Kanász-Nagy, R. Schmidt, F. Grusdt, E. Demler, D. Greif, and M. Greiner, Experimental realization of a long-range antiferromagnet in the Hubbard model with ultracold atoms, Nature (London) **545**, 462 (2017).

[29] H. Bernien, S. Schwartz, A. Keesling, H. Levine, A. Omran, H. Pichler, S. Choi, A. S. Zibrov, M. Endres, M. Greiner, V. Vuletić, and M. D. Lukin, Probing many-body dynamics on a 51-atom quantum simulator, Nature (London) **551**, 579 (2017).

[30] A. Browaeys and T. Lahaye, Many-body physics with individually controlled Rydberg atoms, Nat. Phys. **16**, 132 (2020).

[31] H. Labuhn, D. Barredo, S. Ravets, S. de Léséleuc, T. Macr, T. Lahaye, and A. Browaeys, Tunable two-dimensional arrays of single Rydberg atoms for realizing quantum Ising models, Nature (London) **534**, 667 (2016).

[32] N. Friis, O. Marty, C. Maier, C. Hempel, M. Holzäpfel, P. Jurcevic, M. B. Plenio, M. Huber, C. Roos, R. Blatt, and B. Lanyon, Observation of Entangled States of a Fully Controlled 20-Qubit System, Phys. Rev. X **8**, 021012 (2018).

[33] G. Pagano, A. Bapat, P. Becker, K. S. Collins, A. De, P. W. Hess, H. B. Kaplan, A. Kyprianidis, W. L. Tan, C. Baldwin, L. T. Brady, A. Deshpande, F. Liu, S. Jordan, A. V. Gorshkov, and C. Monroe, Quantum approximate optimization of the long-range Ising model with a trapped-ion quantum simulator, Proc. Natl. Acad. Sci. **117**, 25396 (2020).

[34] J. Venderley, V. Khemani, and E.-A. Kim, Machine Learning Out-of-Equilibrium Phases of Matter, Phys. Rev. Lett. **120**, 257204 (2018).

[35] H. Théveniaut and F. Alet, Neural network setups for a precise detection of the many-body localization transition: Finite-size scaling and limitations, Phys. Rev. B **100**, 224202 (2019).

[36] E. van Nieuwenburg, E. Bairey, and G. Refael, Learning phase transitions from dynamics, Phys. Rev. B **98**, 060301 (2018).

[37] M. Matty, Y. Zhang, Z. Papić, and E.-A. Kim, Multifaceted machine learning of competing orders in disordered interacting systems, Phys. Rev. B **100**, 155141 (2019).

[38] W. Zhang, L. Wang, and Z. Wang, Interpretable machine learning study of the many-body localization transition in disordered quantum Ising spin chains, Phys. Rev. B **99**, 054208 (2019).

[39] D.-L. Deng, X. Li, and S. Das Sarma, Machine learning topological states, Phys. Rev. B **96**, 195145 (2017).

[40] J. F. Rodriguez-Nieva and M. S. Scheurer, Identifying topological order through unsupervised machine learning, Nat. Phys. **15**, 790 (2019).

[41] O. Balabanov and M. Granath, Unsupervised interpretable learning of topological indices invariant under permutations of atomic bands, arXiv:2008.07268.

[42] E. Greplova, A. Valenti, G. Boschung, F. Schäfer, N. Lörch, and S. Huber, Unsupervised identification of topological order using predictive models, arXiv:1910.10124.

[43] T. Vieijra, C. Casert, J. Nys, W. De Neve, J. Haegeman, J. Ryckebusch, and F. Verstraete, Restricted Boltzmann Machines for Quantum States with Non-Abelian or Anyonic Symmetries, Phys. Rev. Lett. **124**, 097201 (2020).

[44] H.-Y. Hu, S.-H. Li, L. Wang, and Y.-Z. You, Machine learning holographic mapping by neural network renormalization group, Phys. Rev. Res. **2**, 023369 (2020).

[45] B. S. Rem, N. Käming, M. Tarnowski, L. Asteria, N. Fläschner, C. Becker, K. Sengstock, and C. Weitenberg, Identifying quantum phase transitions using artificial neural networks on experimental data, Nat. Phys. **15**, 917 (2019).

[46] A. Bohrdt, C. S. Chiu, G. Ji, M. Xu, D. Greif, M. Greiner, E. Demler, F. Grusdt, and M. Knap, Classifying snapshots of the doped Hubbard model with machine learning, Nat. Phys. **15**, 921 (2019).

[47] Y. Zhang, A. Mesaros, K. Fujita, S. D. Edkins, M. H. Hamidian, K. Ch'ng, H. Eisaki, S. Uchida, J. C. S. Davis, E. Khatami *et al.*, Machine learning in electronic-quantum-matter imaging experiments, Nature (London) **570**, 484 (2019).

[48] C. Szegedy, W. Liu, Y. Jia, P. Sermanet, S. Reed, D. Anguelov, D. Erhan, V. Vanhoucke, and A. Rabinovich, Going deeper with convolutions, arXiv:1409.4842.

[49] M. Lin, Q. Chen, and S. Yan, Network in network, arXiv:1312.4400.

[50] C. Miles, A. Bohrdt, R. Wu, C. Chiu, M. Xu, G. Ji, M. Greiner, K. Q. Weinberger, E. Demler, and E.-A. Kim, Correlator convolutional neural networks: An interpretable architecture for image-like quantum matter data, arXiv:2011.03474.

[51] K. Mills, K. Ryczko, I. Luchak, A. Domurad, C. Beeler, and I. Tamblyn, Extensive deep neural networks for transferring small scale learning to large scale systems, Chem. Sci. **10**, 4129 (2019).

[52] D. A. Martin, T. L. Ribeiro, S. A. Cannas, T. S. Grigera, D. Plenz, and D. R. Chialvo, Box-scaling as a proxy of finite-size correlations, arXiv:2007.08236.

[53] G. Vidal, Classical Simulation of Infinite-Size Quantum Lattice Systems in One Spatial Dimension, Phys. Rev. Lett. **98**, 070201 (2007).

[54] F. Chollet *et al.*, Keras, https://keras.io (2015).

[55] See Supplemental Material at http://link.aps.org/supplemental/10.1103/PhysRevResearch.4.L022032 for additional information about network architecture, observables in different bases, and different partitions.

[56] U. Wolff, Collective Monte Carlo Updating for Spin Systems, Phys. Rev. Lett. **62**, 361 (1989).

[57] F. Y. Wu, The Potts model, Rev. Mod. Phys. **54**, 235 (1982).

[58] M. Kardar, *Statistical Physics of Fields* (Cambridge University Press, Cambridge, England, 2007).

[59] S. Sachdev, *Quantum Phase Transitions*, 2nd ed. (Cambridge University Press, Cambridge, England, 2011).

[60] V. R. Vieira, Quantum information and phase transitions: Fidelity and state distinguishability, J. Phys.: Conf. Ser. **213**, 012005 (2010).

[61] S.-J. Gu, Fidelity approach to quantum phase transitions, Int. J. Mod. Phys. B **24**, 4371 (2010).

[62] P. Peczak and D. P. Landau, Monte Carlo study of finite-size effects at a weakly first-order phase transition, Phys. Rev. B **39**, 11932 (1989).

[63] K. Liu, N. Sadoune, N. Rao, J. Greitemann, and L. Pollet, Revealing the phase diagram of Kitaev materials by machine learning: Cooperation and competition between spin liquids, arXiv:2004.14415.

[64] I. Cong, S. Choi, and M. D. Lukin, Quantum convolutional neural networks, Nat. Phys. **15**, 1273 (2019).

[65] H.-Y. Huang, R. Kueng, G. Torlai, V. V. Albert, and J. Preskill, Provably efficient machine learning for quantum many-body problems, arXiv:2106.12627.

[66] A. Seif, M. Hafezi, and C. Jarzynski, Machine learning the thermodynamic arrow of time, Nat. Phys. **17**, 105 (2021).

[67] Y. Zhang and E.-A. Kim, Quantum Loop Topography for Machine Learning, Phys. Rev. Lett. **118**, 216401 (2017).

[68] M. Iqbal and N. Schuch, Entanglement Order Parameters and Critical Behavior for Topological Phase transitions and Beyond, Phys. Rev. X **11**, 041014 (2021).